

ORIGINAL ARTICLE

STUDY OF THE LATENT PHASE OF RADIATION-INDUCED LUNG INJURY

Anna Lierová¹✉, Marcela Jeličová¹, Jaroslav Pejchal² and Zuzana Šinkorová¹

¹ Department of Radiobiology, Faculty of Military Health Sciences, University of Defence, Hradec Kralove, Czech Republic

² Department of Toxicology and Military Pharmacy, Faculty of Military Health Sciences, University of Defence, Hradec Kralove, Czech Republic

Received 2nd April 2020.

Accepted 13th July 2020.

Published 4th December 2020.

Summary

Early changes after radiation exposure may serve as predictors as well as targets for alleviation of radiation-induced injury in the lung. The aim of our study was to examine alterations on the cell and tissue levels in the lung and blood changes of immunological and cytokines profiles induced by ionizing radiation (IR) during the first month after irradiation in the mice experimental model. Female C57BL/6 mice were total body irradiated (TBI) by 8 Gy. Lung tissue samples and blood were collected 4, 8 and 24 h, 7, 21 and 30 d after TBI. We measured absolute cell counts, cell populations and cytokines profile in the blood and evaluated histopathological analysis in the lung, immunophenotypization of the main lung cell populations and cytokine profiles. In blood, the acute radiation syndrome developed with recovery being observed at 21–30 d, observed by hematological markers. In the lung tissue, a biphasic response occurred. At first, a significant decreased of lymphocytes, resident tissues macrophages and air/tissue ratio associated with increased neutrophils was observed at 8 – 24 h. Subsequently, increase in infiltrating CD4⁺ T-lymphocytes, neutrophils and resident tissues macrophages and decreased airiness were measured 21 and 30 d after TBI. In summary, our study describes the mechanisms that lung tissue enables to cope with non-lethal injury.

Key words: ionizing radiation; radiation induced lung damage; radiation pneumonitis; latent phase; lymphocytes; cytokines.

BACKGROUND

Some of the worst health-related consequences from radiation events, are from nuclear power plant accidents or nuclear weapon misuse, have brought an increased attention towards the solution of future threats. On the other hand, the use of ionizing radiation (IR) in the medical or industrial fields has become a common occurrence. Therefore, the field of radiobiology has been developed to address any concern arising from its daily use (1). One of the major goals of radiobiology is to gather and understand the information regarding the development of acute and chronic effects of ionizing radiation exposure. The advances made in clinical case studies showed

✉ University of Defence, Faculty of Military Health Sciences, Department of Radiobiology, Třebešská 1575, 500 01 Hradec Králové, Czech Republic
anna.lierova@unob.cz

that the acute or chronic effects of irradiation can only be explained by a new concept of radiation-induced multi-organ failure (RI-MOF) (2). This concept is supported by the bystander effect, which acts as a “bridge” between the initial acute radiation damage leading to delayed tissue effects (3). The observed outcome in survivors from nuclear events revealed the seriousness of respiratory tract damage, which is exacerbated after the initial manifestation of acute radiation syndrome (4). The lungs are extremely sensitive structures due their complexity and its enriched capillary network, in which >40 different cell types can be identified. Therefore, radiation-induced lung injury (RIPI) typically resolves during the early stages of radiation toxicity (5).

RIPI is typically manifested in two distinct patterns radiation pneumonitis (RP), an early inflammatory phase, and radiation fibrosis (RF), the late chronic phase. Thus, RIPI is a dose-limiting factor for thorax and total body irradiation (TBI) (6). Regardless, thoracic irradiation is performed frequently, especially in cases of lung, breast, mediastinal, and certain rare forms of heart cancer (7). However, these treatments may result in the absorption of ionizing radiation by the surrounding healthy tissue and induce lung toxicity. Concerning TBI, its highest risk comes not from clinical practice but from nuclear events, although it is common procedure before the transplant of allogeneic peripheral blood stem cells in patients with hematologic malignancies (8).

Several RIPI studies suggest a temporal sequence of events, starting with an early “latent” period that may progress into acute RP and/or chronic radiation RF. Therefore, understanding the mechanisms regulating this process is critical in the development of effective radioprotective strategies against RIPI. Moreover, the only interval for effective treatment is found during the latent and acute phases, as the fibrotic lung damage phase results in irreversible and fatal tissue remodeling. The inherent complexity of radiation lung toxicity suggests that blocking or influencing the entire process requires a more comprehensive approach than just targeting one molecular pathway (9) and, so far, only the latent phase interval appears promising in the modulation of RIPI.

The aim of our study was to establish a time course for the cellular and tissue changes in lung after TBI (8 Gy). This dose is just under the lethal dose ($LD_{50/30}$) for C57Bl/6 mice; therefore, a higher dose is impossible due to TBI lethality. In this regard, Johnson et al. (10) indicated that a TBI sub-threshold (0.5 - 10 Gy) significantly increases cytokine expression and that this disbalance is critical for the development of acute and chronic tissue reactions. This study postulates that lung damage as the major component of TBI, resolved from systemic damage due to the impairment of the immune and inflammatory response. Thus, our study enables the exploration of the early cellular and tissue response in the lung after sub-threshold TBI.

MATERIAL AND METHODS

Experimental animals and irradiation

Female C57Bl/6 mice (Velaz, Unetice, Czech Republic) aged 12 – 16 weeks and weighing 20 – 25 g were kept in controlled conditions (22 ± 2 °C, air humidity $50 \pm 10\%$) with a 12 h day cycle, fed with standard ST-1 feed and provided with tap water *ad libitum*. All procedures performed on animals had been approved by the ethics committee of the Faculty of Military Health Sciences in Hradec Kralove. At the beginning of the experiment, the mice were randomly assigned into groups (10 mice per the group).

For irradiation procedure, the animals were kept in a Plexiglas box (VLA JEP, Hradec Kralove, Czech Republic) and totally irradiated with the dose of 8 Gy using a ^{60}Co unit (Chisotron, 1 m distance, dose rate 0.37 Gy/min; Chirana, Prague, Czech Republic). The control group was not irradiated.

Tissue isolation

Mice were euthanized by overdoes of inhalant anesthetics 4, 8 and 24 h, 7, 21 and 30 d after irradiation. Samples from lung and peripheral blood were collected from individual mice. Blood was collected into tubes without anticoagulant (BD Bioscience, Franklin Lakes, NJ, USA) for sera extraction to assess cytokine levels and into heparinized tubes (BD Bioscience) for determination of blood counts and cell populations. The left pulmonary lobe was clamped and taken for histological analyses, while the right lobe of the lung was infused by phosphate buffered saline (PBS; Sigma-Aldrich, St. Louis, MI, USA) to wash off peripheral blood and then divided into two parts,

which were weighed and further processed for flow cytometry and cytokine analysis. Part of harvested tissue intended for cytokine profiling was immediately frozen and stored at -80°C until next processing.

Analysis of cytokine expression

The cytokine profile was determined from the blood sera and the supernatant from lung tissue. Sera were obtained from collected blood. After collection, the whole blood was allow clotting by leaving it undisturbed at room temperature for 45 min and centrifuged. The samples were aliquoted and stored at -80°C until next processing. Lung tissue supernatants were prepared by lysis of tissue in lysis buffer (Cell Signaling Technology, Danvers, MA, USA) containing protease inhibitor cocktail (Roche Diagnostics GmbH, Mannheim, Germany). After 1h incubation, samples were sonicated and centrifuged. The supernatants were collected, aliquoted, and store at -80°C until next processing.

The cytokine profile in sera and tissue supernatants were determined using the commercially available BD™ Cytometric Bead Array Mouse Inflammation Kit (BD Bioscience). The detection was performed on a FACSAria II cell sorter (BD Bioscience). The kit contains polystyrene beads coated with capture antibodies specific for individual cytokines (IL-6, IL-10, IL-12p70, $\text{INF}\gamma$, $\text{TNF}\alpha$, and MCP-1). The prepared samples were processed according to the user's manual supplied by the producer.

Peripheral blood analysis

The heparinized blood was divided into two parts. A volume of 150 μL was designated for blood counts. Blood counts were measured by ABX Pentra 60 C+ haemoanalyzer (Horiba, Kyoto, Japan). The remainder of the blood (approximately 200 – 300 μL) was lysed using EasyLyse™ (Dako, Glostrup, Denmark) and the cell suspension (5×10^5 cells) was marked with a panel of directly labelled monoclonal antibodies for evaluating changes in main lymphocytic populations (T-lymphocytes: anti-mouse directly labelled monoclonal antibodies CD3 ϵ – FITC, T-lymphocyte subpopulations, including T cytotoxic [Tc] cells: CD8 – PECy7 and T helper [Th] cells: CD4 – BV421, B lymphocytes: CD19 – PE, and natural killer cells [NK cells]: NK1.1 – APC). All antibodies used in this experiment were purchased from BD Bioscience or BioLegend (San Diego, CA, USA).

Lung tissue analysis

Pulmonary tissue was designated for monitoring changes in cell populations and was enzymatically digested in Iscove's Modified Dulbecco's Medium (2 mg/mL collagenase + 50 U/mL DNase) at 37°C for 60 min. After digestion, cells were filtered through the strainer (100 μm) to remove tissue debris. The obtained single cell suspensions were subsequently centrifuged, counted in hemocytometer chamber after dilution with Turk's solution (2 % acetic acid) and resolved in PBS for next analysis. The acquired cell suspension was subsequently marked with 2 cocktails of directly labelled monoclonal antibodies. The first cocktail was designed for main lymphocyte populations and subpopulations (the common leukocyte marker CD45 – APC Fire 750 and the same antibodies for lymphocytes subpopulations were used as for blood samples). The second mix included monoclonal antibodies for determination of against myeloid cells (monocytes: Ly6C – FITC, macrophages: F4/80 – PE, neutrophilic granulocytes: Ly-6G – PECy7, alveolar macrophages and dendritic cells: CD11c – BV421, myeloid marker: CD11b – BV510, and CD45 – APC Fire 750). All antibodies used in this experiment were purchased from BD Bioscience or BioLegend.

The lung samples determined for histological examination were fixed with 10% neutral buffered formalin (Paramix, Holice, Czech Republic), embedded into paraffin and 5 μm thick tissue sections were cut (microtome model no. SM2000 R; Leica Microsystems, Heidelberg, Germany). Staining with hematoxylin and eosin (H&E; Merck, Kenilworth, NJ, USA) and histochemical detection of naphthol AS-D chloroacetate (Sigma-Aldrich) positive cells were performed. Air/tissue ratio and cell infiltration were measured by BX-51 microscope equipped with DP-72 camera (both from Olympus, Tokyo, Japan). Air/tissue ratio were evaluated in ten randomly selected viewing fields (excluding bronchi and large vessels) and percent of microscopic fields were calculated by using the Image-Pro 5.1 computer image analysis system (Media Cybernetics Inc., Bethesda, MD, USA) at 200 \times magnification.

Statistics

Data represent mean \pm standard deviation (SD) calculated from ten mice in each group. Statistical analysis was performed using Kruskal-Wallis and post hoc Mann-Whitney tests by IBM SPSS statistics version 24 (IBM, Armonk, NY, USA). Differences were considered significant when $p \leq 0.05$.

RESULTS

Cytokine profiles in blood and lung tissue

Cytokine profiles were determined in blood sera and supernatants from lung tissue. Of all the detected cytokines, only two reached statistically significant differences when compared with control, including IL-6 (Fig. 1A) and MCP-1 (Fig. 1B). IL-6 was significantly higher in both (sera and lung tissues) at 8 h and then only in sera at 7 and 21 d after irradiation. MCP-1 reached significantly increased levels in both samples at 4 h and 7 – 21 d after TBI.

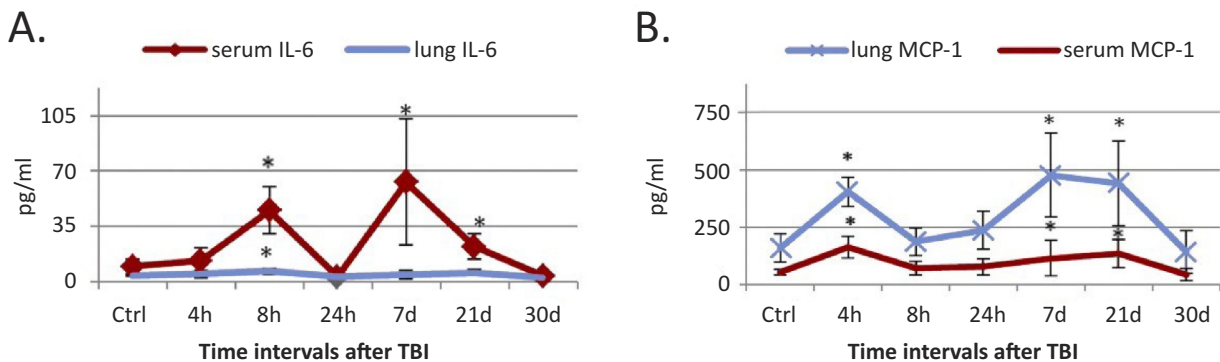


Figure 1. Evaluation of cytokine concentrations in blood sera and lung tissues in different time intervals after 8 Gy TBI. A.) Profile of IL-6. B.) Profile of MCP-1. Statistically significant when compared to the control (Ctrl) * $p \leq 0.05$ group

Blood counts

Blood count changes induced by IR are depicted in Fig. 2A. Lymphocytes significantly decreased 4 h – 21 d after TBI. Monocytes showed a significant decrease at 24 h – 7 d, whereas their numbers significantly increased 21 and 30 d after TBI. Neutrophils showed significant decline at 7 and 21 d after TBI.

Immunophenotyping of leukocyte populations

IR caused changes in leukocyte populations in peripheral blood and lung tissue, especially in lymphocyte populations (Fig. 2B and Fig. 3A, respectively). B-lymphocytes significantly decreased at 4 h – 30 d after TBI. By contrast, T-lymphocytes and NK cells significantly increased in blood 8 h after TBI and then decreased at 24 h – 21 d and 7 – 21 d, respectively. Proportion of individual T-lymphocyte subpopulations (Tc and Th) did not alter during the experiment (data not shown). In the 30 d time-point, all lymphocyte populations started to recover.

In the lung tissues (Fig. 3A), total leukocytes significantly decreased 4 h – 7 d after TBI. Individual leukocyte populations varied with time. Lymphocytes were significantly lower than control in 4 h – 21 d interval, whereas their numbers increased at 30 d, which was mainly due to the infiltration of lung tissue by CD4⁺ Th cells (data not shown). Alveolar macrophages (AM) were characterized by high expression of CD11c and F4/80, but lack CD11b expression what differed them from dendritic cells and interstitial macrophages. AM significantly decreased 4 h – 7 d after TBI. Similarly to lymphocytes, their numbers increased at 30 d. Finally, neutrophils significantly decreased in the 7 d time-point, whereas their infiltration of lung tissue increased 21 – 30 d after TBI.

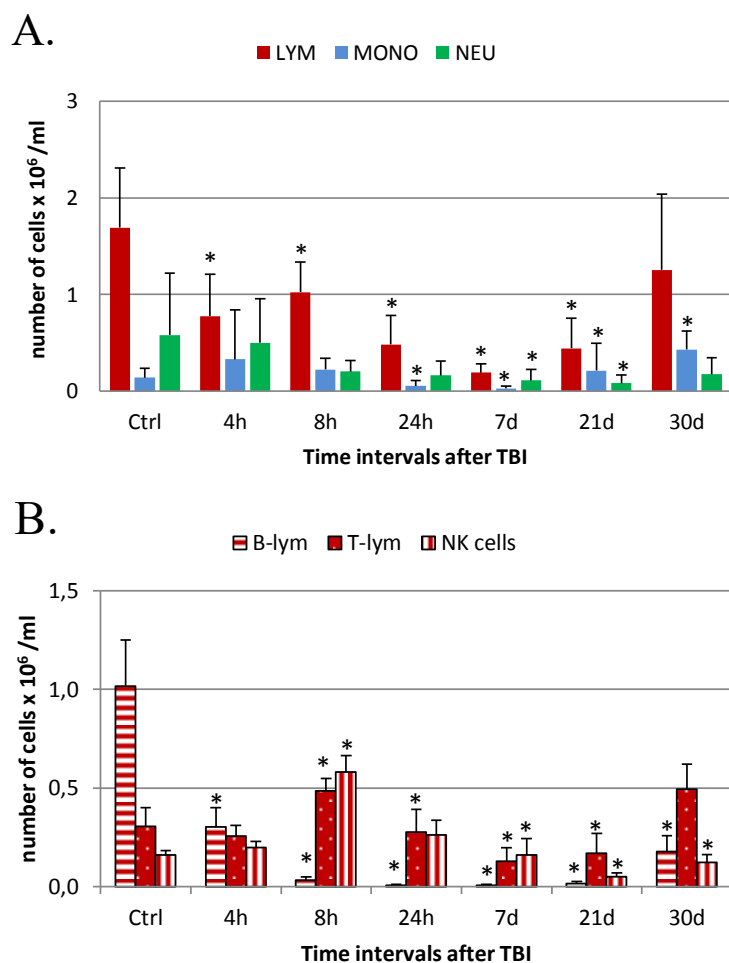


Figure 2. Peripheral blood analyses in different time intervals after 8 Gy TBI. A.) Blood counts. Determination of absolute numbers of lymphocytes (LYM), monocytes (MONO) and neutrophils (NEU). B.) Immunophenotypization of lymphocytes in the blood. Absolute numbers of individual lymphocyte populations: B-lymphocytes (B-lym), T-lymphocytes (T-lym) and natural killer cells (NK cells). Statistically significant when compared to the control (Ctrl): * $p \leq 0.05$

Histological analysis of lung tissues

Results of histological analysis are depicted in Fig. 3. Air/tissue ratio significantly decreased (Fig. 3B), while neutrophil infiltration significantly increased (Fig. 3C) 8 – 24 h and 21 – 30 d after TBI.

DISCUSSION

Exposure to low IR doses from the environment or clinical sources has become the standard of our life. The Atomic Era began in the 50's, when the first nuclear bomb was detonated. Since then, “the fear of radiation” has risen up with increased warnings of nuclear accidents, sabotage or even terrorism. In the case of large-scale radiation events, military services have a critical role in the emergency response. Unexpected TBI in human beings and the systematic response to IR is highly relevant in nuclear events or accidents with lethal or near-lethal TBI. The key task during radiation events is the triage of victims. For military and non-military institutions the need to recognize and evaluate the health hazards of radiation are compiled in the system **Medical Treatment Protocols for Radiation Accident (METREPOL)** (11). This system has been extensively revised due to new RI-MOF concepts after radiation exposure (12). Current research in the field of radiation injuries need to understand the pathophysiology and to identify the prognostic parameters for organic and systemic damage. Further development of diagnostic

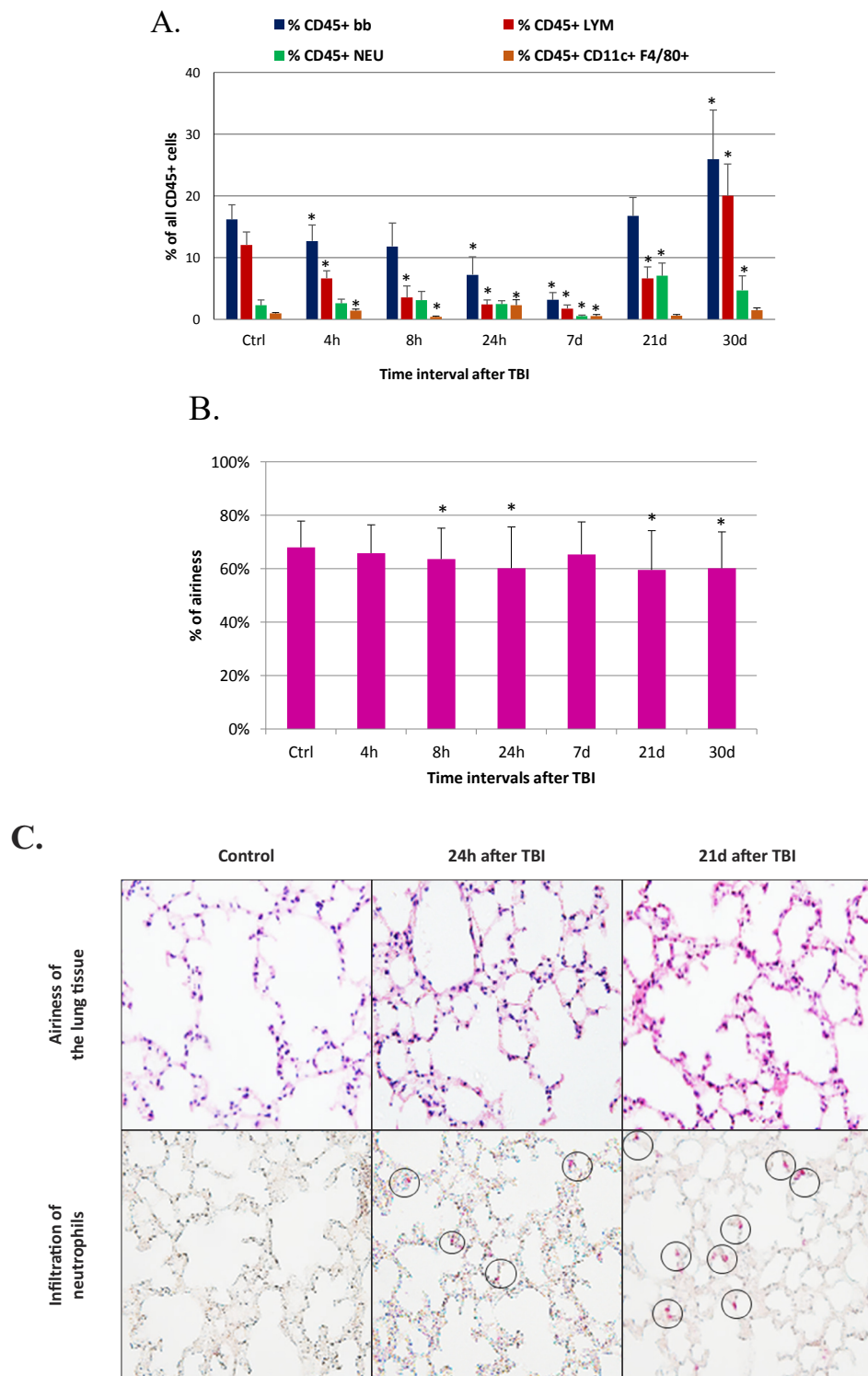


Figure 3. Lung tissue analyses in different time intervals after 8 Gy TBI. **A.)** Immunophenotypization of leukocytes in the lung tissue. Evaluating changes in relative numbers of leukocyte (CD45+) populations: lymphocytes (LYM), alveolar macrophages (CD11c⁺, F4/80⁺), and neutrophilic granulocytes (NEU). **B.)** Determination of lung tissue airiness by hematoxylin and eosin staining. **C.)** Histological and histopathologic analyses of lung tissue. Representative images of hematoxylin and eosin staining and naphthol AS-D chloroacetate histochemical staining of neutrophils. Circles indicate neutrophil presence. Statistically significant when compared to the control (Ctrl): * $p \leq 0.05$

and therapeutic strategies and their assessment in practice require experimental studies to estimate the current METREPOL triage system. Because of the extremely limited numbers of studies from radiological victims, animal models have been more suitable for the development of diagnostic and therapeutic standards. Although it is difficult to extrapolate lung-specific changes, our model may help to understand the alterations in lung tissue in the context of TBI, which significantly worsens prognosis. In our study, we focused on mapping the early changes in blood and lung tissue after TBI with a dose of 8 Gy. In the C57/BL model this dose is close to the LD_{50/30} of the animals and, based on the available literature, it is a suitable model to simulate the organ failure sequence observed during RI-MOF (13).

Several factors have a demonstrated influence in the severity of radiation injuries; among these, cytokine level has been identified as a critical component for late effect progression in the lung tissue (14). An inflammatory reaction is fundamental after radiation exposure and is presumed to play a pivotal role in the development of both acute and delayed radiation responses in many tissues. RIPI begins with a non-specific “cytokine storm” as a result of the immune response upholding the homeostasis and the damaged cells in the irradiated microenvironment (15).

Initially, we observed that the most radiosensitive cells, B-lymphocytes, significantly decreased in number at 4 h after TBI in both tissues, which was accompanied with increased MCP-1 concentration. MCP-1 is produced by a variety of cells, such as macrophages and fibroblasts (16). After irradiation, its expression can be upregulated via NF- κ B signaling (17). MCP-1 functions as a chemoattractant for monocytes, T-lymphocytes, NK cells, and neutrophils into the place of inflammation or injury (18). In our model, MCP-1 may have stimulated the release of Th and NK cells into the bloodstream and their subsequent transition into lung tissue at 8 h (although it was non-significant in the case of Th lymphocytes). Further, it could have simultaneously supported the migration of neutrophils. An Influx of these cells into the lungs affects the integrity of the alveolar-capillary complex, which was demonstrated by decreased air/tissue ratio within an 8 – 24 h interval. IL-6 was also significantly altered during the initial phase. IL-6 is a reactant of the acute phase and a pro-inflammatory cytokine produced by macrophages, neutrophils, hepatocytes, and T-lymphocytes (14). Interestingly, IL-6 production was delayed when compared with MCP-1 and its concentration in blood exceeded its level in the pulmonary tissue, indicating that its source may have been located elsewhere than in the lungs. Increased permeability of a lung alveolar – capillary membrane could also have caused its passive filtration. At 24 h, both MCP-1 and IL-6 returned to baseline levels, which may reflect the progression of DNA repair (19,20).

Thereafter, significant leukopenia was developed in the peripheral blood and lung tissue due to acute hematopoietic radiation syndrome at 7 d. The lack of immune cells most likely stimulates MCP-1 and IL-6 production, which may contribute to bone marrow recovery (21,22).

However, from day 21 we can observe a different radiation damage course in the lung tissue compared to the peripheral blood. In our model, the recovery of immune cells was noticed 21 d after TBI, suggesting the influx of cells into the lung thus impairing the airiness of the tissue. On the other hand, MCP-1 and IL-6 decreased at 30 d. Sub-threshold injury seems to suppress the pro-inflammatory response in the lung tissue in order to achieve homeostasis. In contrast, when the lung tissue was irradiated with lethal doses the cytokine production it was intensified after 30 d in some studies (23,24). Therefore, the inhibition of MCP-1 and IL-6 signaling soon after the recovery phase may contribute to the mitigation of RIPI.

From 21 d, a significant increment in the relative proportion of lymphocytes and neutrophils was observed, reaching maximum on day 30. In this interval, an increased number of already monitored populations were observed. A more detailed analysis of the lymphocyte population revealed that this change is due to the predominance of T-lymphocytes (data not shown). The population of Th-lymphocytes was dominant, as opposed to peripheral blood when both populations recovered similarly. The infiltration of Th-lymphocytes and neutrophils into the lung tissue is one of the characteristic manifestations of the latent phase of RIPI. During this phase, only structural and histopathological changes at the cellular and molecular level can be observed directly in the tissue, although the patient does not present any clinical manifestations. It has been shown that the course and intensity of events in this phase determine the establishment of the whole RIPI process in the tissue. The specific events that occur are mainly radiation-induced loss of type I pneumocytes, ultrastructural changes of lamellar bodies of type II pneumocytes and significant changes in the endothelium of vascular capillaries. The functional subunit of the lung

is the alveolar-capillary barrier which is also the most sensitive subunit to IR. Due to alveolar-capillary barrier damage, an increased number of alveolar macrophages and peripheral immune cells in the lung tissue and swelling of the interstitial space, leading to acute inflammation – radiation pneumonitis (25–27).

Supported by our results, we conclude that lung injury occurring after TBI close to lethal dose manifested differently than the response in experimental models primary intended for RIPI research. RIPI delay manifestation is characteristic for TBI models, with initial molecular and cellular patterns observed as early as 4 – 8 h after irradiation and secondary specific to latent phase manifestation in the lung tissue after 21 – 30 d post irradiation. Consistent results were reported by Johnston et al. (10), but their study did not find any correlation between early increments in cytokines after TBI with doses of 0.5 – 5 Gy and chronic pathological changes. However, a study by Unthank et al. (28) confirmed the significant presence of RF in the lung after 19 months post-TBI with 8.5 – 8.7 Gy. This study also demonstrated significant fibrosis in the heart and kidneys, which may reflect the mechanisms of RI-MOF. The alternations observed in lung tissue demonstrated by current reports introduce the possibility for the modulation of delayed radiation-induced injuries after a sub-lethal TBI dose. Nevertheless, deeper research is needed for the comprehensive understanding of the pathophysiology of RI-MOF and the assignment of improved strategies and protocols not only for nuclear event casualties but for patients of radiation therapy.

In summary, this study demonstrates that the early post-irradiation response at sublethal doses causes significant changes in the lungs; further, it demonstrates that the lungs are radioresistant when compared to the hematopoietic system. The great advantage of our study is that provided the connection between the tissue changes, hematological parameters, population characteristics of lung lymphocytes, and the study of cytokine kinetics. Important findings from our study show a detailed representation of molecular and cellular alternation inducing near-lethal TBI and the subsequent radiation lung toxicities. The demonstrated lung injury during the early stages after TBI was identical with typical molecular and cellular responses described for latent phase of radiation pneumonitis. The lack of data on the sub-threshold lung injury and clear understanding of the mechanisms underlying radiation damage are the reasons why radiation toxicity represents a serious complication. Therapeutic intervention during the early stages after irradiation may reverse the subsequent tissue changes and thus late radiation toxicity.

Funding

This work was supported by the Ministry of Defense of the Czech Republic (Long-term organization development plan, Medical Aspects of Weapons of Mass Destruction of the Faculty of Military Health Sciences, University of Defence) and by the Ministry of Education, Youth and Sport, Czech Republic (Specific Research Project No: SV/FVZ201507).

Declaration of interest

The authors report no conflicts of interest. The authors alone are responsible for the content and writing of the paper.

Adherence to Ethical Standards

All procedures performed on animals had been approved by the ethics committee of the Faculty of Military Health Sciences in Hradec Kralove. This article does not contain any studies involving human participants performed by any of the authors.

REFERENCES

1. Kirsch DG, Diehn M, Kesarwala AH, Maity A, Morgan MA, Schwarz JK, et al. The Future of Radiobiology. *J Natl Cancer Inst.* 01 2018;110(4):329–40.
2. Macià i Garau M, Lucas Calduch A, López EC. Radiobiology of the acute radiation syndrome. *Rep Pract Oncol Radiother.* 6. červenec 2011;16(4):123–30.
3. Marín A, Martín M, Liñán O, Alvarenga F, López M, Fernández L, et al. Bystander effects and radiotherapy. *Rep Pract Oncol Radiother.* 28. srpen 2014;20(1):12–21.

4. Hiram T, Tanosaki S, Kandatsu S, Kuroiwa N, Kamada T, Tsuji H, et al. Initial medical management of patients severely irradiated in the Tokai-mura criticality accident. *Br J Radiol.* duben 2003;76(904):246–53.
5. Coggle JE, Lambert BE, Moores SR. Radiation effects in the lung. *Environ Health Perspect.* prosinec 1986;70:261–91.
6. Fleckenstein K, Zgonjanin L, Chen L, Rabbani Z, Jackson IL, Thrasher B, et al. Temporal Onset of Hypoxia and Oxidative Stress After Pulmonary Irradiation. *International Journal of Radiation Oncology*Biophysics*Physics.* 1. květen 2007;68(1):196–204.
7. Formenti SC, Demaria S. Systemic effects of local radiotherapy. *Lancet Oncol.* červenec 2009;10(7):718–26.
8. Goans RE, Wald N. Radiation accidents with multi-organ failure in the United States. *BJR.* 1. leden 2005;Supplement_27(1):41–6.
9. Tsoutsou PG, Koukourakis MI. Radiation pneumonitis and fibrosis: Mechanisms underlying its pathogenesis and implications for future research. *International Journal of Radiation Oncology*Biophysics*Physics.* 1. prosinec 2006;66(5):1281–93.
10. Johnston CJ, Manning C, Hernady E, Reed C, Thurston SW, Finkelstein JN, et al. Effect of total body irradiation on late lung effects: hidden dangers. *Int J Radiat Biol.* srpen 2011;87(8):902–13.
11. Flidner TM, Friessecke I, Beyrer K, editoři. *Medical Management of Radiation Accidents: Manual on the Acute Radiation Syndrome.* London: British Institute of Radiology; 2001. 64 s.
12. Flidner TM, Dörr HD, Meineke V. Multi-organ involvement as a pathogenetic principle of the radiation syndromes: a study involving 110 case histories documented in SEARCH and classified as the bases of haematopoietic indicators of effect. *BJR.* 1. leden 2005;78(Supplement 27, 1):1–8.
13. Williams JP, McBride WH. After the bomb drops: A new look at radiation-induced multiple organ dysfunction syndrome (MODS). *Int J Radiat Biol.* srpen 2011;87(8):851–68.
14. Lierova A, Jelcova M, Nemcova M, Proksova M, Pejchal J, Zarybnicka L, et al. Cytokines and radiation-induced pulmonary injuries. *J Radiat Res.* 1. listopad 2018;59(6):709–53.
15. Tálas M, Szolgay E, Várterész V, Koczás G. Influence of acute and fractional X-irradiation on induction of interferon in vivo. *Arch Gesamte Virusforsch.* 1972;38(2):143–8.
16. Yadav A, Saini V, Arora S. MCP-1: chemoattractant with a role beyond immunity: a review. *Clin Chim Acta.* 11. listopad 2010;411(21–22):1570–9.
17. Manna K, Das U, Das D, Kesh SB, Khan A, Chakraborty A, et al. Naringin inhibits gamma radiation-induced oxidative DNA damage and inflammation, by modulating p53 and NF-κB signaling pathways in murine splenocytes. *Free Radic Res.* duben 2015;49(4):422–39.
18. Malik IA, Moriconi F, Sheikh N, Naz N, Khan S, Dudas J, et al. Single-Dose Gamma-Irradiation Induces Up-Regulation of Chemokine Gene Expression and Recruitment of Granulocytes into the Portal Area but Not into Other Regions of Rat Hepatic Tissue. *Am J Pathol.* duben 2010;176(4):1801–15.
19. Horn S, Barnard S, Rothkamm K. Gamma-H2AX-Based Dose Estimation for Whole and Partial Body Radiation Exposure. *PLoS One* [Internet]. 23. září 2011 [citován 18. duben 2019];6(9). Dostupné z: <https://www.ncbi.nlm.nih.gov/pmc/articles/PMC3179476/>
20. Wirsdörfer F, Jendrossek V. Modeling DNA damage-induced pneumopathy in mice: insight from danger signaling cascades. *Radiat Oncol.* 24. srpen 2017;12(1):142.
21. Xu YX, Talati BR, Janakiraman N, Chapman RA, Gautam SC. Growth Factors: Production of Monocyte Chemotactic Protein-1 (MCP-1/JE) by Bone Marrow Stromal Cells: Effect on the Migration and Proliferation of Hematopoietic Progenitor Cells. *Hematology.* 1999;4(4):345–56.
22. Kovacević-Filipović M, Petakov M, Hermitte F, Debeissat C, Krstić A, Jovčić G, et al. Interleukin-6 (IL-6) and low O(2) concentration (1%) synergize to improve the maintenance of hematopoietic stem cells (pre-CFC). *J Cell Physiol.* červenec 2007;212(1):68–75.
23. Rube CE, Wilfert F, Palm J, König J, Burdak-Rothkamm S, Liu L, et al. Irradiation Induces a Biphasic Expression of Pro-Inflammatory Cytokines in the Lung. *Strahlenther Onkol.* 1. červenec 2004;180(7):442–8.
24. Chen B, Na F, Yang H, Li R, Li M, Sun X, et al. Ethyl pyruvate alleviates radiation-induced lung injury in mice. *Biomed Pharmacother.* srpen 2017;92:468–78.
25. Morgan GW, Pharm B, Breit SN. Radiation and the lung: A reevaluation of the mechanisms mediating pulmonary injury. *International Journal of Radiation Oncology*Biophysics*Physics.* 15. leden 1995;31(2):361–9.
26. Ghafoori P, Marks LB, Vujaskovic Z, Kelsey CR. Radiation-induced lung injury. Assessment, management, and prevention. *Oncology (Williston Park, NY).* leden 2008;22(1):37–47; discussion 52-53.

27. Ding N-H, Li JJ, Sun L-Q. Molecular Mechanisms and Treatment of Radiation-Induced Lung Fibrosis. *Curr Drug Targets*. říjen 2013;14(11):1347–56.
28. Unthank JL, Miller SJ, Quickery AK, Ferguson EL, Wang M, Sampson CH, et al. Delayed Effects of Acute Radiation Exposure in a Murine Model of the H-ARS: Multiple-Organ Injury Consequent to <10 Gy Total Body Irradiation. *Health Phys*. listopad 2015;109(5):511–21.